This article has been accepted for publication in a future issue of this journal, but has not been fully edited. Content may change prior to final publication. Citation information: DOI 10.1109/TTE.2020.3028784, IEEE Transactions on Transportation Electrification

Lithium Battery State of Health Estimation via Differential Thermal Voltammetry with Gaussian Process Regression

Zhenpo Wang, *Member, IEEE*, Changgui Yuan, Xiaoyu Li, *Student Member, IEEE*

***Abstract*—Accurate state of health estimation can give valuable guidelines for improving the reliability and safety of energy storage system. Herein, a novel battery degradation tracking method is proposed through fusion significant health features with Gaussian process regression. First, an advanced filter method is used to smooth differential thermal voltammetry curves. Thereafter, considering the relationship between battery degradation and differential thermal voltammetry curves, some health factors are extracted from differential thermal voltammetry curves. Here, these health factors involve different dimensions of differential thermal voltammetry curve including peak position, peak and valley values. Third, a correlation analysis method is employed to select four high-quality features from health factors, which are fed into Gaussian process regression to learn and establish battery degradation model. Finally, the estimation accuracy, robustness and reliability of proposed model are verified using four batteries with different aging test conditions and health levels. The results demonstrate that the proposed model can provide accurate battery health status forecasting.**

***Index Terms*—Lithium-ion batteries, state of health, differential thermal voltammetry, Gaussian regression process.**

I. INTRODUCTION

LITHIUM battery has become the primary energy storage forms for micro-scale portable equipment and macro-scale transportation, energy storage system in modern society because it has many advantageous performances such as high energy and power densities, long cycle life [1-3]. However, these advantageous features will be degraded with various operation environments. The scenarios easily lead to battery system failure even more occur fire and explosive accidents. Hence, it is necessary to predict and know the battery current status for improving reliability and stability of battery system. Developing non-destructive technology and knowledge is a critical challenge in battery health research through external characteristics such as voltage, current and temperature [4, 5].

Currently, battery health research focuses on short-term state of health (SOH) and long-term remaining useful lifetime (RUL) based on the different time-scales [6, 7]. Reviewing amounts of literature, the approaches of short-term SOH estimation are primary analysis of the collected external battery parameters. While the models of battery RUL prediction are mainly based on sampled historical capacity data [8]. After that, the empirical-based and machine learning-based methods are applied to building battery model. Roughly, the empirical-based methods mainly capture the changes of physical characteristics with battery degradation such as internal resistance [9]. The machine learning-based methods take advantage of advanced algorithms and computational tools to map the relationship between battery health features (HFs) and battery health levels. Otherwise, considering battery belongs to complex physicochemistry system, some electrochemical analysis techniques are proposed to research battery degradation. Therefore, the battery health condition prognostic can be summarized four manners: (1) empirical-based methods; (2) model-based methods; (3) machine learning-based methods; and (4) feature signal analysis methods.

1) Empirical-based methods: The approach needs large laboratory test data to analyze the correlation between battery capacity fade and stress factors such as resistance, temperature and depth-of-discharging (DOD). Based on the battery aging pathways, the method can be concluded as calendar aging and cyclic aging models. The main variables are time, temperature and storage SOC in calendar aging model. Considering battery storage temperature and time, the calendar aging model appears to follow the Arrhenius-like kinetic [10, 11]. Introducing another stress factor of battery storage SOC, the Tafel equation fusion with a novel calendar lifetime prediction model is proposed and the calendar semi-empirical model combines with the impedance-based electro-thermal model for achieving complete lifetime model [12]. The cycle aging involves complex external environment factors that typically consider the voltage, current, temperature and DOD. Some traditional cycle aging models are established by using the cycle number, cumulative charge capacity and current rate [13]. Considering the relationship between lithium loss and Coulombic efficiency, the convex degradation trend of lithium battery is effectively captured and a semi-empirical model is proposed [14]. Under different state-of-charge (SOC) ranges, lithium battery aging

Manuscript received 17-May-2020; revised 06-Aug-2020 and 25-Sep-2020; accepted 30-Sep-2020. This work was supported in part by the National Key R&D Program of China under (Grant 2018YFB0105700), in part by the Scholarship from the China Scholarship Council and in part Graduate Technological Innovation Project of Beijing Institute of Technology. (Corresponding authors: Xiaoyu Li, xiaoyu_li187@163.com).

Z. Wang, C. Yuan, X. Li and are with the National Engineering Laboratory for Electric Vehicles, School of Mechanical Engineering, Beijing Institute of Technology, Beijing 100081, China.

2332-7782 (c) 2020 IEEE. Personal use is permitted, but republication/redistribution requires IEEE permission. See http://www.ieee.org/publications_standards/publications/rights/index.html for more information.
Authorized licensed use limited to: University Library Utrecht. Downloaded on October 21,2020 at 08:15:30 UTC from IEEE Xplore. Restrictions apply.

This article has been accepted for publication in a future issue of this journal, but has not been fully edited. Content may change prior to final publication. Citation information: DOI 10.1109/TTE.2020.3028784, IEEE Transactions on Transportation Electrification

mechanisms are fitted using a simple semi-empirical function [15-17]. These battery degradation models can simplify and easily implement in some specific scenarios. However, battery degradation conditions are influenced by many stress factors, hence the prognostic accuracy is limited due to the models cannot consider comprehensive and multivariable factors.

2) Model-based methods: To analyze the relationship between resistances with capacity fade, the empirical-based physical model named equivalent circuit model (ECM) are used to obtain the actual resistances of battery through least square method or/and its extended forms. Based on ECM, some scholars proposed co-estimation for battery SOC and SOH [18, 19]. Chen et al. proposed genetic algorithm (GA) to identify battery parameters under various driving cycles and these parameters are applied to estimate battery health conditions [20]. Otherwise, the sequence resistances are employed to analyze battery long-term degradation. Yu at al. used multiscale logic regression algorithm to predict battery RUL using moved windows [21]. Meanwhile, Wei et al. fitted battery resistance series with polynomial function and the polynomial regression is employed to forecast battery long-term RUL [17, 22]. Summary, the empirical-based physical model has many advantages and can construct concise framework for forecasting battery health conditions. However, the results easily suffer from noises perturbations that primarily depend on the robustness and reliability of these selected algorithms and models.

3) Machine learning-based methods: The methods are regarded as well-known technologies involving probability theory, statistics, convex analysis and complexity theory that are applied in various fields such as data mining, computer vision, and natural language processing for modeling and simulating. Therefore, some machine learning methods such as support vector machine (SVM), Gaussian process regression (GPR) and neural network (NN) are utilized to establish battery degradation model for mapping battery capacity fade with HFs. Chen et al. used radial basis SVM method to model battery degradation through analyzing based on battery partial charge voltage and current data [23]. Li at al. proposed dual-GPR framework to establish battery degradation models for estimation battery short-term SOH and long-term RUL, respectively [8, 24]. Dai et al. proposed a prior knowledge-based neural network (PKNN) and the Markov chain method to predict battery SOH according to multiple features of aging battery [25]. In addition, with ever-increasing the cloud computing and big data technologies, the multidimensional and practical battery data are collected that will give enormous potentials for machine learning-based methods. However, selecting and extracting high-quality training features are time-consuming from massive amounts of operational data. Hence, it is necessary to develop some manners to obtain features of battery degradation.

4) Feature signal analysis methods: To extract appropriate and reliable battery degradation features, some methods such as incremental capacity analysis (ICA), differential voltage analysis (DVA) and differential thermal voltammetry (DTV) are proposed based on electrochemistry analysis techniques [26, 27]. ICA method mainly captures the capacity-changed rate in specific voltage intervals for analyzing battery aging and material characteristics. Normally, the peaks of IC curves are gradually toward to lower left with battery aging during the charging tested process [28, 29]. DVA method can analyze battery aging by considering two inflection points and these points also shift with the increased cycle number of battery aging test [30]. The two methods mentioned above both are popular in prognostic battery health conditions. Li at al. proposed dual-GPR framework to establish battery degradation models for estimation battery short-term SOH and long-term RUL through combining IC features with GPR algorithm [8, 24]. Weng et al. proposed a battery SOH monitoring framework through fusing partial IC curves with support vector regression (SVR) [31]. Li et al. used random forest regression (RFR) algorithm to establish battery degradation model through extracting battery health features from charging voltage [32]. DTV method has been validated and applied to track battery health conditions considering the correlation between battery surface temperatures and capacity degradation. Wu et al. proposed a low-cost battery health diagnostic method by analyzing the changes of entropic heats [33, 34]. Otherwise, these methods integrate with machine learning algorithms are used to improve the accuracy of forecasting battery health conditions. Motivating by this thought, the targets of this work to propose a framework fusion machine learning with DTV analysis method to forecast battery degradation conditions.

The main contributions of this study are forecasting battery capacity degradation through merging data-driven and signal processing methods. In this framework, a novel method of battery actual available capacity prediction is established using GPR algorithm with the features of DTV curves. Specifically, an advanced filter method is employed to smooth the raw DTV curves. Six health factors are extracted from the curves considering peak position, peak and valley values at first. Secondly, the general correlation analysis method is applied to obtain strong-correlation features as health performance indicators. Then a modified kernel GPR-based algorithm is utilized to model battery degradation for SOH estimation. Finally, the proposed method of battery SOH estimation is verified in two cases using four battery datasets from NASA data repository. Otherwise, this work is mainly an offline method at present, but it will have huge potential application values with the development of cloud technology and multiple data are applied in the xEVs. In real-world applications, this work provides a pre-research and guidance for the future design of prediction method, when the data collection and cloud technology is combined with the onboard BMS.

The rest of this paper is organized as follows: Section II introduces battery aging phenomena and differential thermal voltammetry analysis. Section III is the proposed framework and specific modeling methodology. Section IV presents the results and discussions of the proposed method for two cases. The key conclusions are summarized in Section V.

II. BATTERY AGING PHENOMENA AND DIFFERENTIAL THERMAL VOLTAMMETRY ANALYSIS

In this study, the four batteries are carried out under regular cycle aging experiment and the detailed tested schedules at first are described in part A. After that, the means of obtaining the smooth DTV curves are introduced in part B. Then the specific

2332-7782 (c) 2020 IEEE. Personal use is permitted, but republication/redistribution requires IEEE permission. See http://www.ieee.org/publications_standards/publications/rights/index.html for more information.
Authorized licensed use limited to: University Library Utrecht. Downloaded on October 21,2020 at 08:15:30 UTC from IEEE Xplore. Restrictions apply.

This article has been accepted for publication in a future issue of this journal, but has not been fully edited. Content may change prior to final publication. Citation information: DOI 10.1109/TTE.2020.3028784, IEEE Transactions on Transportation Electrification

methods of feature extraction are detailed discussed and high-correlation features are analyzed and presented in part C.

A. Battery Aging Experimental Data Analysis

Four tested data of four batteries are labeled No.5, No.6, No.7, and No.18, which are the second-generation18650-size lithium batteries with the same composite materials (LiCoO2), are obtained from the NASA Ames Prognostics Center of Excellence [35]. The degradation experiment of the four batteries is tested under three schemes including constant-current and constant-voltage charge (CC-CV) mode, constant current (CC) discharge at room temperature (24℃). The upper cut-off voltages of four batteries are 4.2V for the four batteries during charging process, respectively. The four batteries charge with the same CC-CV modes and the evolution curves of current, temperature and voltage are described in Fig. 1(a). Here the charging current keeps 1.5A until the corresponding voltage reaches to upper cut-off voltage of 4.2V. Hereafter, the charging process stops when the charging current below to 20mA during the CV period. The temperature can be divided into three parts based on the current load modes. After that, the four batteries discharge with continued current 2A until the voltages reach the preset values 2.7V, 2.5V, 2.2V and 2.5V for battery No.5, No.6, No.7, and No.18, respectively.

As illustrated in Fig. 1(b), the trends of capacities decrease with cycle number for the four batteries. Due to the reversible properties, the phenomena of battery capacity have some regenerations. Hence, the capacity degradation curves are not in monotone decreasing trends. This nonlinear relationship leads to higher technical requirements for forecasting health conditions. Some robust and accurate features are imperative to extract from the battery external parameters and construct a reliable battery degradation model. The detailed experimental conditions are summarized in Table. I. And the feature extraction and application are description in the next part.

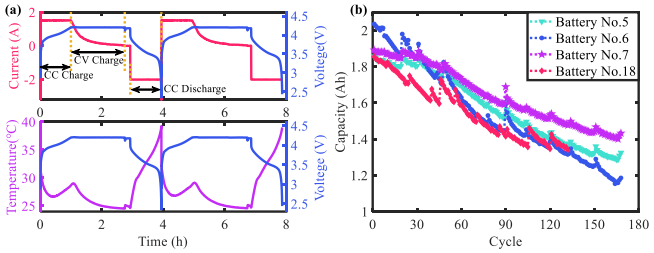

Fig. 1. The battery aging cycle schemes and capacity degradation profiles: (a) A completed aging cycle test for voltage and current; (b) capacity degradation curves of the four batteries.

Table. I. The four batteries' specific cycle condition

Battery label	Batteries' cycle condition				
	Charging cut-off voltage (V)	Discharging cut-off voltage (V)	Charging constant current (A)	Discharging current (A)	Temperature (ºC)
No.5	4.2	2.7	1.5	2	24
No.6	4.2	2.5	1.5	2	24
No.7	4.2	2.2	1.5	2	24
No.18	4.2	2.5	1.5	2	24

B. Differential Thermal Voltammetry Analysis and Filter

Battery degradation contains complex physicochemical process cannot capture the accurate health levels through easily measured parameters and little computation cost. Larges of battery degradation data together with fundamental understanding in battery aging indicate that entropic changes have significant correlation in analysis battery degradation. Entropic changes can regard as rates of temperatures changes since entropy is a specific function of temperature. Considering the entropic changes coupling with battery system, DTV analysis method, combining with the external voltage and temperature parameters during galvanostatic charge/discharge, is proposed. The method can easily implement that requires only two external collected parameters in controlled environment. DTV can be calculated by the ratio of the temperature and voltage differentials as follows,

$$DTV = \frac{dT}{dt} \Big/ \frac{dV}{dt} = \frac{dT}{dV} \tag{1}$$

where T and t refer to the battery surface temperature and sample time, respectively. V is the terminal voltage of the battery. From the Eq. (1), the inversely proportional to dV/dt demonstrates that the voltage intervals have significant impacts on DTV values. As we know, the voltages will keep constant in different sample times, or may lead to divergence. Meanwhile, the significant features may be submerged at large voltage intervals and are vulnerable to noise pollution at small voltage intervals, as shown in Fig. 2(a). In this work, the voltage interval is set as 5mV based on trial and error to get good results.

To avoid these problems, some advanced filter methods are employed to obtain effective DTV curves for extraction significant features. The smooth results of two general filter methods named moving averaging (MA) and Savitzky-Golay (SG) filter are analyzed and compared. MA is normally used for time series data to smooth short-term fluctuations and highlight longer-term trends. The filter thresholds are defined by the actual short-term and long-term application. Specifically, the method uses a fixed moving window size N is selected to smooth the original data. The MA method is described as follows,

$$Y(i) = \frac{1}{N}\sum_{j=0}^{N-1} X(i+j) \tag{2}$$

where $X(\cdot)$ is the input initial sample signals and $Y(\cdot)$ is the output signal. N is the fixed window size of the series. From the Eq. (2), the filter capability mainly relies on window size and neighbors' data. Hence, the random measured noise and impulse response signal can be smoothed using the MA method. Nevertheless, it is difficult to find suitable sizes for various filter conditions and that time-consuming to choose the size.

SG filter was first presented in 1964 by Abraham Savitzky and Marcel J. E. Golay [36], which is widely applied to data smoothing with excellence property in high-frequency digital signal filter. The algorithm is a time-domain filter method based on local least-squares polynomial approximation algorithm [37]. The most attractive characteristics of the SG filter are maintained the shape and height of waveform peaks. In fact, the method can hold the low-frequency signal data while removing related high-frequency part, which has many advantages for filtering the DTV curves to obtain high-quality features. The simple construction of the filter is described as follows,

$$Y(i) = \sum_{j=-m}^{j=m} \frac{1}{N} C_j X(i+j) \tag{3}$$

The fundamental function is similar to MA method, where $X(i)$ is the original input signals and Cj is the coefficient given

2332-7782 (c) 2020 IEEE. Personal use is permitted, but republication/redistribution requires IEEE permission. See http://www.ieee.org/publications_standards/publications/rights/index.html for more information.
Authorized licensed use limited to: University Library Utrecht. Downloaded on October 21,2020 at 08:15:30 UTC from IEEE Xplore. Restrictions apply.

This article has been accepted for publication in a future issue of this journal, but has not been fully edited. Content may change prior to final publication. Citation information: DOI 10.1109/TTE.2020.3028784, IEEE Transactions on Transportation Electrification

by the SG filter, and *F(·)* is the resultant output signals. *N* refers to the number of convoluting integers, which is equal to the smoothing window size *(2m+1)*. The detailed calculation process of the filter method is listed in Table II.

Compared with the MA method, the primary contribution of the SG filter method is to use a least-square method to obtain corresponding coefficients to fit its neighbors and smooth each sample point. In this work, the used SG filter method can not only ensure to obtain smooth the curves, but also can get more steady curves in the head and the tail of the DTV curve. Hence, the method can provide important features information for battery health estimation in the future step. From Fig. 2(a), the results of the two methods for smoothing the original DTV curves in the first cycle of the battery No.6. Obviously, the initial DTV curve has similar smoothed results using both the two filter methods. However, SG filter method has steadier filter effect in the zoom figure, which has prominent performance in capturing the peak points from the DTV curve. Thus, this work the SG method is employed to smooth the DTV curves. To evaluate the two different filter methods, here the basic mathematical thought of smoothness is introduced. Specifically, in mathematical analysis, the smoothness of a function is a property measured by the number of continuous derivatives. Hence, the results of two filtered DTV curves are able to be evaluated using the differential methods. As shown in Fig. 2(b), we compared the differential of SG-based DTV curve with the differential of MA-based DTV curve. Obviously, the differential curve of SG-based method has small fluctuations, which means the SG-based method can give an excellent filter performance. Therefore, the results of SG-based filter method are superior to the MA-based for these tested batteries and the SG-based method is applied to the four batteries for extracting battery health features.

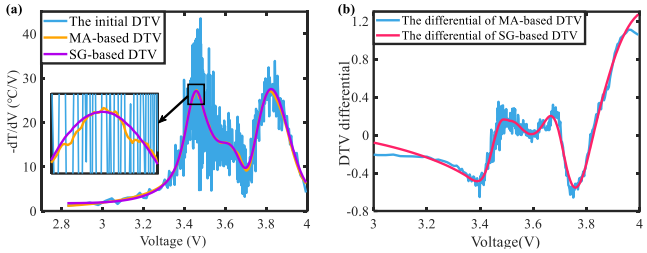

Fig. 2. The DTV curve of battery No.6. (a) the comparison of DTV curves smoothed by Savitzky-Golay and Moving average methods; (b) evaluation the two different filter methods using battery No.6.

Table. II. The Savitzky-Golay Filter

(1) Initialization

$$N = 2m+1$$

$$x = [x_{-m}, x_{-m+1}, \ldots, x_{m-1}, x_m]$$

(2) Fit data points by polynomial

$$y_i = a_0 + a_1 x_i + a_2 x_i^{\ 2} + \ldots + a_{k-1} x_i^{\ k-1}$$

$$Y_{(2m+1)\times 1} = X_{(2m+1)\times k} \cdot A_{k\times 1} + E_{(2m+1)\times 1}$$

(3) Least squares solution of A

$$\dot{A} = (X^T \cdot X)^{-1} \cdot X^T \cdot Y$$

(4) The filtering result of Y

$$\dot{Y} = X \cdot A = X \cdot (X^T \cdot X)^{-1} \cdot X^T \cdot Y$$

C. Features extraction of battery degradation based on correlation analysis method

Battery degradation can be regarded as complex process, the battery internal chemical/physical properties have gradually changed such as electrolyte solvent reducing, internal resistance increasing, and normal voltage decreasing and result in battery capacity fade. The DTV analysis method as an effective and easy technique is used to reflect the battery degradation conditions. During the actual operation process, the current profile of battery has little opportunity in fully charging/discharging situation. Hence, it is difficult to get completed DTV curves in the engineering application. Considering primary voltage range of actual operation, here some significant features of DTV curves are extracted based voltage range (3.2 to 4.0V) to express battery health condition and to build battery degradation model. In this work, six features are extracted from different degrees of DTV curves such as peak position, peak and valley values. Therefore, it is imperative to pick up the peak and valley points in DTV curves. Then the corresponding voltages and DTV values can be obtained based on the relationship between voltage and DTV. The specific mathematic descriptions of peak and valley can be expressed as follows,

$$\begin{cases} V_{peak} = V_i \Big|_{\frac{dDTV}{dV_i}=0 \ and \ f(V_i) \geq f(V), V \in (V_i - w, V_i + w)} \\ DTV_{peak} = f(V_{peak}) \end{cases} \quad (4)$$

$$\begin{cases} V_{valley} = V_i \Big|_{\frac{dDTV}{dV_i}=0 \ and \ f(V_i) \leq f(V), V \in (V_i - w, V_i + w)} \\ DTV_{valley} = f(V_{valley}) \end{cases} \quad (5)$$

where the Eq. (4) and (5) refer to the battery health features in peak and valley, and the *w* is voltage interval equals to 3mV. The battery health features are denoted as *F* matrix as follows,

$$F = [V_{peak}^1, DTV_{peak}^1, V_{valley}, DTV_{valley}, V_{peak}^2, DTV_{peak}^2] \quad (6)$$

To reduce computational burden and improve robustness of the model, high-quality input datasets of the feature variables are screening through the Pearson correlation analysis method. The strong correlational features are selected as the input datasets for battery degradation model. The specific formula of Pearson's correlation coefficient as follows,

$$r_{xy} = \frac{\sum_{i=1}^{n}(Y_i - \bar{Y})(F_i - \bar{F})}{\sqrt{\sum_{i=1}^{n}(Y_i - \bar{Y})^2}\sqrt{\sum_{i=1}^{n}(F_i - \bar{F})^2}} \quad (7)$$

$$\bar{F} = \frac{1}{n}\sum_{i=1}^{n} F_i \quad (8)$$

where *n* is the number of sample series and here it is total battery cycle number, the F_i refers to the sample points of individual feature variables indexed with *i* and $\bar{F}$ denotes the mean of each type of features. In this study, Y_i is the battery capacity series and $\bar{F}$ is capacity mean, respectively.

Here, the filtered DTV curves at intervals of 30 cycles are applied to illustrate battery degradation conditions, as shown in Fig. 3. Fig. 3(a) shows completed DTV curves that cover almost

2332-7782 (c) 2020 IEEE. Personal use is permitted, but republication/redistribution requires IEEE permission. See http://www.ieee.org/publications_standards/publications/rights/index.html for more information.
Authorized licensed use limited to: University Library Utrecht. Downloaded on October 21,2020 at 08:15:30 UTC from IEEE Xplore. Restrictions apply.

This article has been accepted for publication in a future issue of this journal, but has not been fully edited. Content may change prior to final publication. Citation information: DOI 10.1109/TTE.2020.3028784, IEEE Transactions on Transportation Electrification

fully discharging process and the voltage ranges from around 2.8V to 4.2V. It is obvious that the trends of DTV curves are moving to left top in the first peaks and the second peaks are moving to bottom left with the increased battery aging cycles. Meanwhile, the valleys between two peaks also obvious changes. These distinct changes of the DTV curves fasten on voltage range from 3.2V and 4.0V and this voltage ranges cover the primary discharged capacity for different battery health conditions. In addition, considering the actual application, all batteries are used in a shallow dis/charging principle, which not only can prolong battery lifespan but also can improve the safety and reliability. Hence, the voltage region is treated as an important area for mapping battery aging. For the sake of capturing effective and robust features, six features are extracted from different degrees of DTV curves such as peak position, peak and valley values. The Pearson correlation analysis method is applied to obtain strong-correlation features for modeling battery degradation. The primary six types of feature variables have been plotted in Fig. 3(b) and Fig. 3(c). The change trends of six feature variables with the battery cycle number are described in Fig. 3(d). Based on the Pearson correlation analysis method, the results of the correlation analysis for the four tested batteries are listed in Table III. As illustration in Table III, compared the results of the FV1 to FV6, the first four FVs have strong correlation with trend of battery capacity degradation. Thus, the four FVs are employed to build battery degradation model.

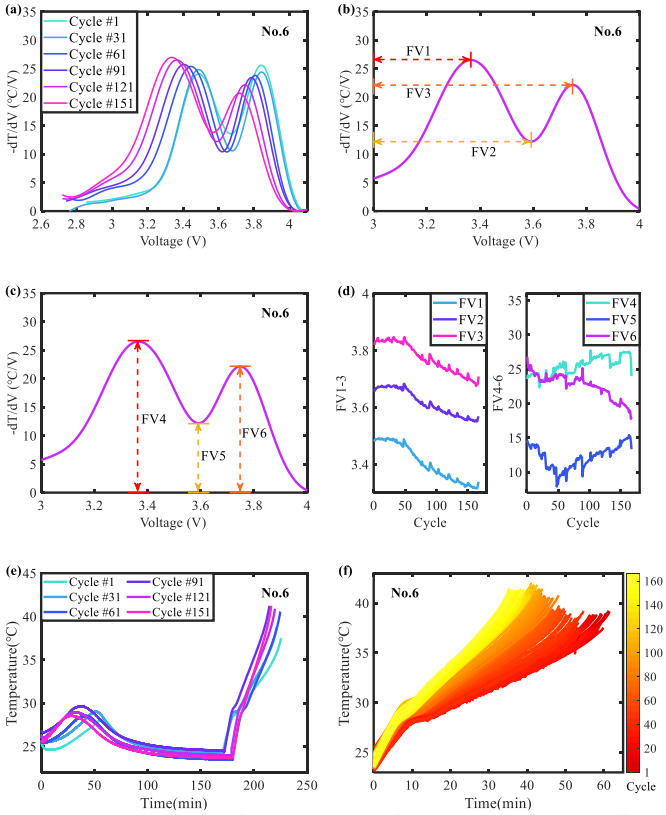

Fig. 3. The DTV curves and feature variables of the battery No.6 under different cycles. (a) The completed DTV curves under different cycles; (b) the features (FV1, FV2 and FV3) extraction from DTV curves under different cycles; (c) the features (FV4, FV5 and FV6) extraction from DTV curves under different cycles; (d) the extraction features with the cycle number, (e) the temperatures of discharging/charging processes under some cycles; (f) the temperatures of different discharging processes.

It is worth noting that the FV is abbreviation of feature variable in this Table. To further explain the relationship between the changes of surface temperature and battery degradation, the temperatures of discharging process have been presented under different cycles, as shown in Fig 3(e). From Fig. 3(f), it can be easily seen that the battery surface temperatures are increasing with cycle number. Therefore, the battery surface temperatures can be regarded as significant indicators for forecasting battery degradation.

Table. III. The detailed results of correlation analysis for the four batteries

	FV1	FV2	FV3	FV4	FV5	FV6
No.5	0.96	0.91	0.94	0.82	0.24	0.57
No.6	0.98	0.96	0.96	0.83	0.33	0.84
No.7	0.93	0.82	0.89	0.77	0.29	0.65
No.18	0.95	0.82	0.89	0.52	0.47	0.84

III. METHODOLOGY

Theory and principle of GPR have been developed over the last decades that has strong competition in many advanced algorithms for many real supervised learning applications [38, 39]. GPR has advantages for high-complexity problems with low computational burden. Hence, the algorithm is unutilized to solve the complex nonlinear problem of battery degradation process and provide an effective model for prognostic battery health conditions.

Known the actual available capacity not only can ensure the safety and reliability for energy storage systems but also can provide valuable parameters for users and manufacturers. Here the primary aim of this work is to construct a capacity prediction model of battery degradation according to external physical parameters such as voltage, temperature and current. Considering the relationship between surface temperature and terminal voltage of battery and capacity degradation, the significant feature variables are analyzed through battery DTV curves.

GPR-based model of battery capacity prediction is established based on these mentioned above features and the detailed extraction method has been introduced in section II. The input feature variables such as peaks position, peak and valley values, which are collected as $\mathbf{X}= [\mathbf{x}_1, \mathbf{x}_2 \ldots, \mathbf{x}_n]$ where $\mathbf{x}_i$ is a four-dimensional vector and the sequences n is the cycle number of tested battery. The output observation values are the series of battery available capacities during battery degradation process. In the GPR-based model, the algorithm primarily consists of mean function $m(\mathbf{x})$ and covariance function $k_f(\mathbf{x}, \mathbf{x}')$, as shown in Eq. (9) and (10).

$$m(\mathbf{x}) = \mathrm{E}\left[f(\mathbf{x}) \right] \tag{9}$$

$$k_f(\mathbf{x}, \mathbf{x}') = \mathrm{E}\left[(f(\mathbf{x}) - m(\mathbf{x}))(f(\mathbf{x}') - m(\mathbf{x}'))^T \right] \tag{10}$$

where $f(\mathbf{x})$ is the target output and $\mathbf{x}$ is d-dimensional n input vectors. The mean function represents the central trend of $f(\mathbf{x})$ and the covariance function refers the shape and structure of $f(\mathbf{x})$. The corresponding Gaussian process is expressed as

$$f(\mathbf{x}) \sim \mathcal{GP}\left(m(\mathbf{x}), k_f(\mathbf{x}, \mathbf{x}') \right) \tag{11}$$

In Eq. (11), the kernel function $k_f(\mathbf{x},\mathbf{x}')$ has significant function in modeling process, which can obtain the prior assumptions for the properties of the underlying latent function.

2332-7782 (c) 2020 IEEE. Personal use is permitted, but republication/redistribution requires IEEE permission. See http://www.ieee.org/publications_standards/publications/rights/index.html for more information.
Authorized licensed use limited to: University Library Utrecht. Downloaded on October 21,2020 at 08:15:30 UTC from IEEE Xplore. Restrictions apply.

This article has been accepted for publication in a future issue of this journal, but has not been fully edited. Content may change prior to final publication. Citation information: DOI 10.1109/TTE.2020.3028784, IEEE Transactions on Transportation Electrification

Generally, the mean function is set as zero and the covariance function uses the Matérn kernel that has the specific form as,

$$k_f(\|\mathbf{x}-\mathbf{x}'\|)=\frac{2^{1-\nu}}{\Gamma(\nu)}\left(\sqrt{2\nu}\frac{\|\mathbf{x}-\mathbf{x}'\|}{\rho}\right)^{\nu}K_\nu\left(\sqrt{2\nu}\frac{\|\mathbf{x}-\mathbf{x}'\|}{\rho}\right),\quad \rho,\nu>0 \tag{12}$$

here Γ and K_ν refer to the gamma function and the second type modified Bessel function, respectively. ρ and ν both are non-negative parameters of the covariance. In real-world, the output of the proposed model with some noises that can be expressed as follows,

$$\mathbf{y}=f(\mathbf{x})+\varepsilon \tag{13}$$

where the noise vector is $\varepsilon=\{\varepsilon_1,\varepsilon_2,\varepsilon_3,\cdots\varepsilon_N\}$. The prior distribution of observations can be denoted as below,

$$\mathbf{y}\sim\mathcal{N}\left(0,\mathbf{K}_f(\mathbf{x},\mathbf{x})+\sigma_n^2\mathbf{I}_n\right) \tag{14}$$

$$\begin{cases}\mathbf{K}_f(\mathbf{x},\mathbf{x})=\left(k_{ij}\right)_{n\times n}\\ k_{ij}=\sigma_f^2\exp\left(-\frac{1}{2}(x_i-x_j)^2P^{-1}\right)\end{cases} \tag{15}$$

in Eq. (14), $\mathbf{K}_f(\mathbf{x}, \mathbf{x})$ and $\mathbf{I}_n$ are both *d*-dimensional matrixes and defined as symmetric positive definite matrix and unit matrix, respectively. $\sigma_n^2\mathbf{I}_n$ denotes as the noise covariance matrix. In Eq. (15), the equation k_{ij} is related to the variables x_i and x_j, which is increasing with a similar degree of the two variables.

To predict the target variable, here given test dataset $\mathbf{x}^*$ and corresponding observation function $\mathbf{y}^*$ couple with the joint prior distribution observation in Eq. (14), which is described as below,

$$\begin{bmatrix}\mathbf{y}\\ \mathbf{y}^*\end{bmatrix}\sim\mathcal{N}\left(0,\begin{bmatrix}\mathbf{K}_f(\mathbf{x},\mathbf{x})+\sigma_n^2\mathbf{I}_n & \mathbf{K}_f(\mathbf{x},\mathbf{x}^*)\\ \mathbf{K}_f(\mathbf{x},\mathbf{x}^*)^T & \mathbf{K}_f(\mathbf{x}^*,\mathbf{x}^*)\end{bmatrix}\right) \tag{16}$$

According to the joint Gaussian prior distribution on $\mathbf{y}$, the posterior distribution of $p(\mathbf{y}^*|\mathbf{x}, \mathbf{y}, \mathbf{x}^*)$ is can be calculated as below,

$$p(\mathbf{y}^*|\mathbf{x},\mathbf{y},\mathbf{x}^*)=\mathcal{N}\left(\mathbf{y}^*|\hat{\mathbf{y}}^*,\sigma^2(\mathbf{y}^*)\right) \tag{17}$$

here the prediction mean and covariance $\hat{\mathbf{y}}^*, \sigma^2(\mathbf{y}^*)$ are given as,

$$\hat{\mathbf{y}}^*=\mathbf{K}_f(\mathbf{x},\mathbf{x}^*)^T\left[\mathbf{K}_f(\mathbf{x},\mathbf{x})+\sigma_n^2\mathbf{I}_n\right]^{-1}\mathbf{y} \tag{18}$$

$$\sigma^2(\mathbf{y}^*)=\mathbf{K}_f(\mathbf{x}^*,\mathbf{x}^*)-\mathbf{K}_f(\mathbf{x},\mathbf{x}^*)^T[\mathbf{K}_f(\mathbf{x},\mathbf{x})+\sigma_n^2\mathbf{I}_n]^{-1}\mathbf{K}_f(\mathbf{x},\mathbf{x}^*) \tag{19}$$

where $\mathbf{K}_f(\mathbf{x}, \mathbf{x}^*)$ is covariance combining training data with test data. In order to execute the process of model prediction, here the hyper-parameters set $\Theta=[\sigma_f, l, \sigma_n]$ are solved and optimized by minimizing the negative log marginal likelihood (NLML) as

$$\Theta_{\text{opt}}=\arg\min_{\Theta}\text{NLML} \tag{20}$$

where

$$\begin{aligned}\text{NLML}&=-\log p(\mathbf{y}|\mathbf{x},\Theta)=\frac{1}{2}\mathbf{y}^T[\mathbf{K}_f(\mathbf{x},\mathbf{x})+\sigma_n^2\mathbf{I}_n]^{-1}\mathbf{y}\\&+\frac{1}{2}\log(\det(\mathbf{K}_f(\mathbf{x},\mathbf{x})+\sigma_n^2\mathbf{I}_n))+\frac{n}{2}\log 2\pi\end{aligned} \tag{21}$$

To solve the Eq. (20), one kind of gradient descent algorithm named partial derivatives of the marginal likelihood is used. The solution procedure as

$$\begin{cases}\dfrac{\partial}{\partial\Theta_i}\log p(\mathbf{y}|\mathbf{x},\Theta)=\dfrac{1}{2}\left\{\left[\alpha y\alpha^T y-\alpha\dfrac{\partial\alpha^{-1}}{\partial\Theta_i}\right]\right\}\\ \alpha=(\mathbf{K}_f(\mathbf{x},\mathbf{x})+\sigma_n^2\mathbf{I}_n)^{-1}\end{cases} \tag{22}$$

When the hyper-parameters are determined, the completed process of establishing the GPR model is finished. To evaluate the performance of the proposed model, the 95% confidence interval (CI) is calculated by the above Eq. (18) and (19) as follows,

$$95\%CI_C=\hat{y}_i^*\pm1.96\times\sigma^2(y_i^*) \tag{23}$$

where the 95% CI represents the under-or over-confident in this range of the results of battery health estimation, respectively. To quantitative analysis the error, two evaluation approaches named mean absolute error (MAE) and the root mean square error (RMSE) are proposed as follows,

$$MAE=\frac{1}{N}\sum_{i=1}^{N}|y_i-\bar{y}_i^*| \tag{24}$$

$$RMSE=\sqrt{\frac{1}{N}\sum_{i=1}^{N}(y_i-\bar{y}_i^*)^2} \tag{25}$$

where $\bar{y}^*$ and y_i are the battery SOH estimation result and real measured value, respectively. *N* refers to the total number of battery aging test.

The specific framework of the proposed GPR-based model of battery SOH estimation is presented in Fig. 4. The framework is divided into feature selection and battery SOH estimation two parts. In the first part, the voltage and temperature are used to obtain smooth DTV curves by SG filter method. Hereafter, the significant features are extracted from the curves by analyzing the peak and valley of these curves. Then these features are regarded as input dataset for modeling battery degradation process based on GPR algorithm. The detailed processes of testing and training model also present in this framework. At last, the results of test datasets are evaluated and analyzed through four error analysis methods.

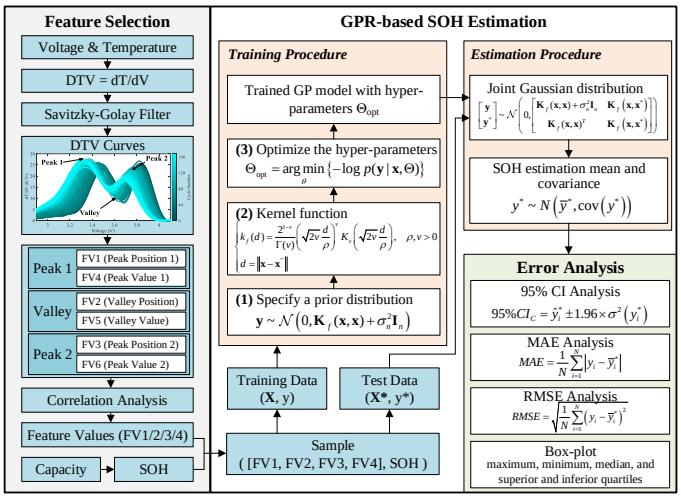

Fig. 4. The framework of the GPR-based battery SOH estimation

2332-7782 (c) 2020 IEEE. Personal use is permitted, but republication/redistribution requires IEEE permission. See http://www.ieee.org/publications_standards/publications/rights/index.html for more information.
Authorized licensed use limited to: University Library Utrecht. Downloaded on October 21,2020 at 08:15:30 UTC from IEEE Xplore. Restrictions apply.

This article has been accepted for publication in a future issue of this journal, but has not been fully edited. Content may change prior to final publication. Citation information: DOI 10.1109/TTE.2020.3028784, IEEE Transactions on Transportation Electrification

IV. SUBMISSION OF FINAL MANUSCRIPT

The proposed method of battery SOH estimation is verified and analyzed in this section. Four batteries datasets are collected from NASA database are used to evaluated accuracy and effectiveness of the GPR-based model at first. Then the robustness and accuracy of the model are further verification by using different initial health conditions in two cases. At last, the performances of the proposed model are discussed using different error analysis methods.

A. Case 1: Battery SOH estimation based on the proposed model

Here four batteries labeled No.5, No.6, No.7 and No.18 are employed to evaluate the accuracy of battery SOH estimation. The four batteries all experience different aging test conditions and the detailed tested profiles are introduced in section II. The significant features combining with corresponding battery capacities construct effective datasets for training and testing of GPR-based model. The first 20% datasets of each battery are treated as training datasets and the remaining for testing and validation. We have presented the results and errors of SOH estimation for the four batteries, as shown in Fig. 5. In this part, all tested batteries are from the first cycle and the values of initial SOHs start from 1 according to the fundamental definition. From Fig. 5, there exist three legends named “Real SOH”, “Estimation SOH” and “95% Confidence Interval” for analysis results of the proposed model. “Real SOH” refers to the actual battery health level based on aging experiment and “Estimation SOH” is the estimation results of the proposed GPR-based model. “95% Confidence Interval” can reflect the uncertainty of the proposed model such as over-estimation and under-estimation.

The detailed results of battery SOH estimation and relative error for each individual battery are shown in Fig. 5. It is worth noting that the four batteries all undergo different aging tests, which represent normal driving condition and over-discharging condition in actual application. From Fig. 5(a) and (b), the results of battery SOH estimation have better accuracy and stability. With the ever-increasing aging cycle tested, the nonlinear trends of capacity degradation become stronger. The situation leads to accuracy decreasing and confidence intervals enlarging during the battery testing process. Fig. 5(b) shows that the relative errors increase with cycle number but the maximum relative error around 1% for the battery No.5. From Fig. 5(c), the estimation results of battery No.6 have larger 95% CI in the terminal of capacity degradation tendency. In-depth analysis, the battery is carried out under over-discharging aging test, which extreme test condition may result in strong nonlinear problem. In Fig. 5(d), the relative errors of the proposed model are also close to 1% for the battery No.6. The battery No.7 has accurate estimation results and the maximum relative error almost 1%, as shown in Figs. 5(e) and (f). For the battery No.18, its capacity series has prominent fluctuation around the EOL compared with other three batteries but the confidence interval is in a narrow range, as shown in Fig. 5(g). The situation reflects the proposed model has high accuracy and reliability. Hence, the relative errors of the battery are all less than 1%, as shown in Fig. 5(h). To sum up, the proposed method for battery SOH estimation has high accuracy for this verification condition.

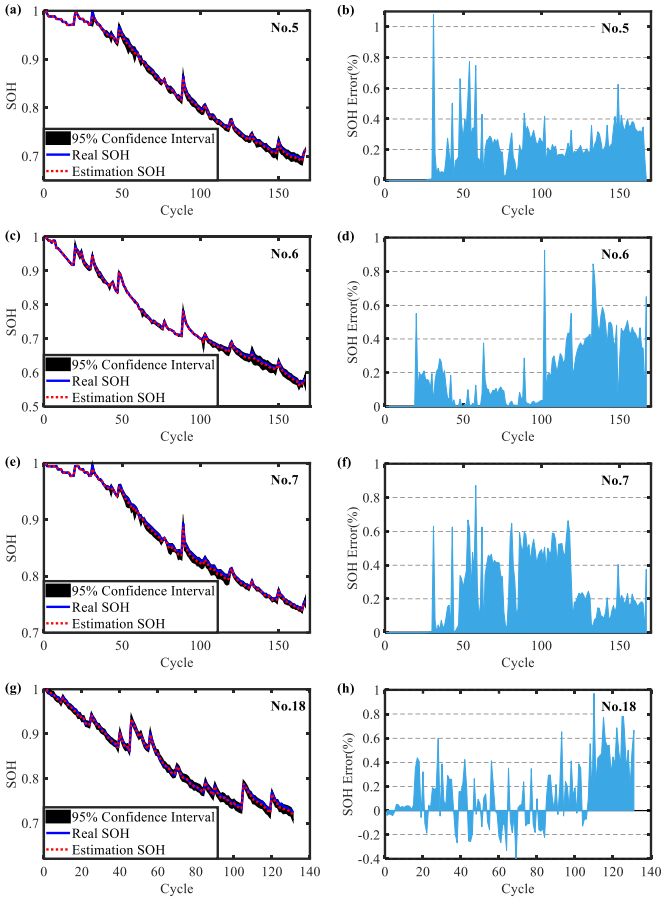

Fig. 5. The proposed GPR-based model for Battery SOH estimation: (a) SOH estimation results for battery No.5. (b) SOH estimation error for battery No.5. (c) SOH estimation result for battery No.6. (d) SOH estimation error for battery No.6. (e) SOH estimation result for battery No.7. (f) SOH estimation error for battery No.7. (g) SOH estimation result for battery No.18. (h) SOH estimation error for battery No.18.

B. Case 2: Verification the robustness of GPR-based models for battery SOH estimation

To verify the robustness and reliability of the proposed GPR-based model, a specific condition with different starting health levels of the tested batteries is designed in this section. Specifically speaking, all datasets of four batteries are collected from any starting cycle, for instance, the 40th cycle in this work. Fig. 6 shows the results of SOH estimations and relative errors for the four batteries. From Fig. 6(a), the estimation results of battery No.5 have better accuracy and the narrower confidence intervals, which states that the proposed model is reliability. Meanwhile, the relative errors are all less than 1% during the completely tested period, as shown in Fig. 6(b). Fig. 6(c) shows the results of battery No.6 and the results indicate the degradation model has higher reliability in training and testing stages according to the 95% CI. From Fig. 6(d), the relative errors are within 1.5% except two points are close to 1.2% because of the capacities impulsion regeneration. Figs. 6(e-h) show that the proposed model has high accuracy and stability. All relative errors are around 1% in this case.

2332-7782 (c) 2020 IEEE. Personal use is permitted, but republication/redistribution requires IEEE permission. See http://www.ieee.org/publications_standards/publications/rights/index.html for more information.
Authorized licensed use limited to: University Library Utrecht. Downloaded on October 21,2020 at 08:15:30 UTC from IEEE Xplore. Restrictions apply.

This article has been accepted for publication in a future issue of this journal, but has not been fully edited. Content may change prior to final publication. Citation information: DOI 10.1109/TTE.2020.3028784, IEEE Transactions on Transportation Electrification

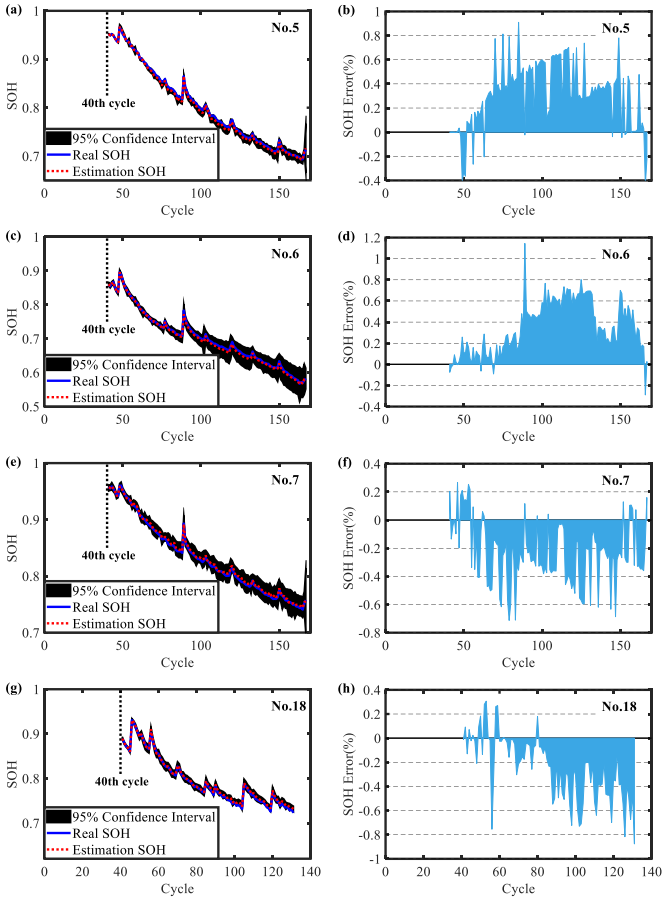

Fig. 6. The proposed GPR-based model for Battery SOH estimation: (a) SOH estimation results for battery No.5. (b) SOH estimation error for battery No.5. (c) SOH estimation result for battery No.6. (d) SOH estimation error for battery No.6. (e) SOH estimation result for battery No.7. (f) SOH estimation error for battery No.7. (g) SOH estimation result for battery No.18. (h) SOH estimation error for battery No.18.

C. Error analysis of GPR-based models for the two cases

Lastly, the errors of the proposed battery degradation model are analyzed for mentioned two cases using through the MAE, RMSE and boxplot, as shown in Fig. 7. Here, MAE is the mean of the absolute difference between the actual measurement and estimation SOH, which can evaluate the rough levels of proposed method. However, the primary disadvantage of MAE is insensitive to outliers. However, RMSE is the square root for the mean of squared errors, which can compensate for the drawback of MAE. As shown in Figs. 7(a) and (b), the results of MAE and RMSE analyses are compared and evaluated in two cases, where the case 1 are better than case 2 in both two analyses. Meanwhile, the results of MAE and RMSE are all less than 0.5%, which indicate that the proposed method has high accuracy and robustness.

Compared with MAE and RMSE analyses, the boxplot can intuitive presentation the conditions of error distribution by avoiding the influences of extreme anomalies. Figs. 7(c) and (d) show the results of boxplot analyses for case 1 and case 2 respectively, and describe the characteristics of error distributions through maximum, minimum, median, and superior and inferior quartiles. From Fig. 7(c), the results of inferior quartile are around 0.15% and the results of superior quartile are close to 0.4% as well as medians concentrate on 0.26% for the tested four batteries. According to the error analyses, the results of battery SOH estimation have small errors indicate the proposed method has excellent accuracy in this case. In Fig. 7(d), the results of inferior and superior quartiles are range from 0.2% to 0.5% and medians concentrate on 0.36% for the tested four batteries in this case. Summary, all results of error analyses demonstrate that the proposed method has high robustness and accuracy under different battery health conditions.

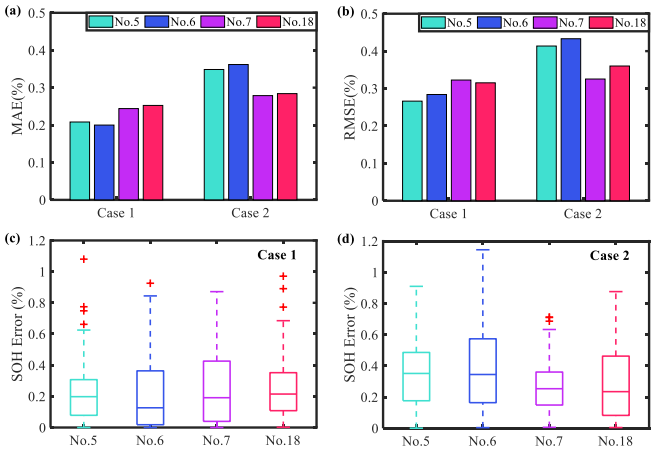

Fig. 7. The error analyses of proposed method for battery SOH estimation: (a) the results of MAE analysis for two cases; (b) the results of RMSE analysis for two cases; (c) the results of boxplot analysis for four batteries in case 1; (d) the results of boxplot analysis for four batteries in case 2.

D. Compared with existing technology based on constant voltage charging (CVC) curve

In this section, to verify the accuracy of the proposed method, the proposed DTV-based method compares with another CVC-based method for battery SOH estimation. The CVC-based method focuses on the constant-voltage (CV) profile of the CC-CV charging step. With the battery aging phenomena, the charging current curves of CV mode have obvious decreasing trends. The ECM is applied to characterize the dynamic behaviors of the aging battery during the CV charging profile [40, 41]. Hence, some health factors are extracted from the ECM in the CV segment for estimating battery SOH. Compared the proposed method with the existing prognostic methods to verify the superiority on the prediction results in Section IV [40], the tested data is the same as this study that both collect from NASA battery database.

The final results of CVC-based methods and the proposed method are shown in Fig. 8. From Fig. 8(a), the maximum MAEs of the three batteries for the two different SOH estimation methods are 1.46% and 0.24%, respectively. Specifically, the maximum MAE (0.24%) of proposed DTV-based method of the three batteries are less than the minimum MAE (0.88%) of the compared CVC-based method. As shown in Fig. 8(b), the maximum RMSEs of the tested batteries are 0.32% and 1.8% for the two methods, respectively. The minimum RMSE of the compared CVC-based method is 1.11%, while the RMSEs of the proposed DTV-based method are all within 0.4%. The error analysis methods indicate that the proposed DTV-based method can give an accurate and effective SOH results.

2332-7782 (c) 2020 IEEE. Personal use is permitted, but republication/redistribution requires IEEE permission. See http://www.ieee.org/publications_standards/publications/rights/index.html for more information.
Authorized licensed use limited to: University Library Utrecht. Downloaded on October 21,2020 at 08:15:30 UTC from IEEE Xplore. Restrictions apply.

This article has been accepted for publication in a future issue of this journal, but has not been fully edited. Content may change prior to final publication. Citation information: DOI 10.1109/TTE.2020.3028784, IEEE Transactions on Transportation Electrification

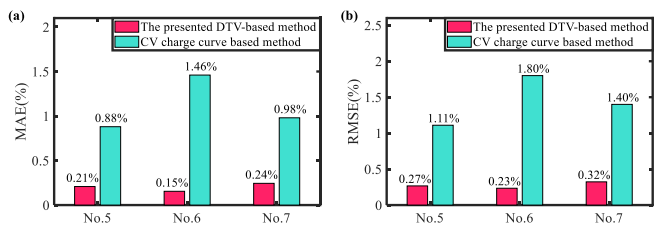

Fig. 8. Compare the proposed method with the existing prognostic methods

V. Conclusion

SOH estimation is one of key functions in various state prognostics for the sake of providing valuable parameter to ensure safety and stability of energy storage system. Flexible and simplified estimation techniques are necessary to achieve accurate and real-time state estimation. However, it is difficult to directly obtain battery state online, since battery is a complex physicochemical system. Here, we proposed a novel battery degradation tracking method based on battery two basic external parameters. The main contributions are summarized as follows: (1) DTV curves are applied to analyze battery health condition under different depth of discharging aging test. (2) Compared with the popular MA filter method, the advanced SG filter method is utilized to smooth DTV curves. (3) The significant feature variables are extracted from DTV curves considering the peak position, peak and valley values, which are regarded as input dataset for battery degradation model. (4) A modified kernel GPR algorithm is applied to establish battery degradation model and analyze the model uncertainty using 95% CI. (5) Two cases of different initial health conditions are designed to verify the proposed model and the various error methods are used to analyze the model. The results demonstrate that the GPR-based model has prominent accuracy and robustness and the maximum relative error within 2%. The proposed method gives different views to capture battery health condition, which no longer collects external information such as load current. The primary limitation of this method maybe not suitable for some special application surroundings. In the future, with the continuous improvement of data acquisition technology and the combination of cloud technology and BEVs, this work will show valuable improvements for the battery SOH prediction. Furthermover, the current model should be considered to update some relevant parameters for giving an accurate, time-saving and universal battery degradation model.

Acknowledgment

This work was supported in part by the National Key R&D Program of China under (Grant 2018YFB0105700), in part by the Scholarship from the China Scholarship Council and in part Graduate Technological Innovation Project of Beijing Institute of Technology (Grant No. 2019CX20021).

References

[1] Y. Feng, C. Xue, Q. Han, F. Han, J. Du, "Robust Estimation for State-of-Charge and State-of-Health of Lithium-ion Batteries Using Integral-Type Terminal Sliding-Mode Observers," IEEE Transactions on Industrial Electronics, pp. 1-1, 2019.

[2] Z. Yang, D. Patil, B. Fahimi, "Online Estimation of Capacity Fade and Power Fade of Lithium-Ion Batteries Based on Input-Output Response Technique," Ieee Transactions on Transportation Electrification, vol. 4, no. 1, pp. 147-156, 2018.

[3] Y. Wang, G. Gao, X. Li, Z. Chen, "A fractional-order model-based state estimation approach for lithium-ion battery and ultra-capacitor hybrid power source system considering load trajectory," Journal of Power Sources, vol. 449, pp. 227543, 2020.

[4] T. Shibagaki, Y. Merla, G. J. Offer, "Tracking degradation in lithium iron phosphate batteries using differential thermal voltammetry," Journal of Power Sources, vol. 374, pp. 188-195, 2018.

[5] Z. Chen, X. Shu, R. Xiao, W. Yan, Y. Liu, J. Shen, "Optimal charging strategy design for lithium-ion batteries considering minimization of temperature rise and energy loss," International Journal of Energy Research, vol. 43, no. 9, pp. 4344-4358, 2019.

[6] X. Li, Z. Wang, L. Zhang, C. Zou, D. D. Dorrell, "State-of-health estimation for Li-ion batteries by combing the incremental capacity analysis method with grey relational analysis," Journal of Power Sources, vol. 410-411, pp. 106-114, 2019.

[7] G. Dong, Z. Chen, J. Wei, "Sequential Monte Carlo filter for state of charge estimation of lithium-ion batteries based on auto regressive exogenous model," IEEE Transactions on Industrial Electronics, pp. 1-1, 2019.

[8] X. Li, Z. Wang, J. Yan, "Prognostic health condition for lithium battery using the partial incremental capacity and Gaussian process regression," Journal of Power Sources, vol. 421, pp. 56-67, 2019.

[9] H. Pan, Z. Lü, H. Wang, H. Wei, L. Chen, "Novel battery state-of-health online estimation method using multiple health indicators and an extreme learning machine," Energy, vol. 160, pp. 466-477, 2018.

[10] I. Bloom, B. W. Cole, J. J. Sohn, S. A. Jones, E. G. Polzin, V. S. Battaglia, G. L. Henriksen, C. Motloch, R. Richardson, T. Unkelhaeuser, D. Ingersoll, H. L. Case, "An accelerated calendar and cycle life study of Li-ion cells," Journal of Power Sources, vol. 101, no. 2, pp. 238-247, 2001.

[11] Y. Wang, Z. Chen, "A framework for state-of-charge and remaining discharge time prediction using unscented particle filter," Applied Energy, vol. 260, pp. 114324, 2020.

[12] M. Ecker, J. B. Gerschler, J. Vogel, S. Käbitz, F. Hust, P. Dechent, D. U. Sauer, "Development of a lifetime prediction model for lithium-ion batteries based on extended accelerated aging test data," Journal of Power Sources, vol. 215, pp. 248-257, 2012.

[13] E. Sarasketa-Zabala, I. Gandiaga, L. M. Rodriguez-Martinez, I. Villarreal, "Calendar ageing analysis of a LiFePO4/graphite cell with dynamic model validations: Towards realistic lifetime predictions," Journal of Power Sources, vol. 272, pp. 45-57, 2014.

[14] F. Yang, X. Song, G. Dong, K.-L. Tsui, "A coulombic efficiency-based model for prognostics and health estimation of lithium-ion batteries," Energy, vol. 171, pp. 1173-1182, 2019.

[15] J. Park, W. A. Appiah, S. Byun, D. Jin, M.-H. Ryou, Y. M. Lee, "Semi-empirical long-term cycle life model coupled with an electrolyte depletion function for large-format graphite/LiFePO4 lithium-ion batteries," Journal of Power Sources, vol. 365, pp. 257-265, 2017.

[16] Y. Wang, C. Liu, R. Pan, Z. Chen, "Modeling and state-of-charge prediction of lithium-ion battery and ultracapacitor hybrids with a co-estimator," Energy, vol. 121, pp. 739-750, 2017.

[17] X. Li, C. Yuan, Z. Wang, "Multi-time-scale framework for prognostic health condition of lithium battery using modified Gaussian process regression and nonlinear regression," Journal of Power Sources, vol. 467, pp. 228358, 2020.

[18] X. Li, Z. Wang, L. Zhang, "Co-estimation of capacity and state-of-charge for lithium-ion batteries in electric vehicles," Energy, vol. 174, pp. 33-44, 2019.

[19] X. Hu, H. Yuan, C. Zou, Z. Li, L. Zhang, "Co-Estimation of State of Charge and State of Health for Lithium-Ion Batteries Based on Fractional-Order Calculus," IEEE Transactions on Vehicular Technology, vol. 67, no. 11, pp. 10319-10329, 2018.

[20] Z. Chen, C. C. Mi, Y. Fu, J. Xu, X. Gong, "Online battery state of health estimation based on Genetic Algorithm for electric and hybrid vehicle applications," Journal of Power Sources, vol. 240, pp. 184-192, 2013.

[21] J. Yu, "State of health prediction of lithium-ion batteries: Multiscale logic regression and Gaussian process regression ensemble," Reliability Engineering & System Safety, vol. 174, pp. 82-95, 2018.

[22] J. Wei, G. Dong, Z. Chen, "Remaining Useful Life Prediction and State of Health Diagnosis for Lithium-Ion Batteries Using Particle Filter and Support Vector Regression," IEEE Transactions on Industrial Electronics, vol. 65, no. 7, pp. 5634-5643, 2018.

2332-7782 (c) 2020 IEEE. Personal use is permitted, but republication/redistribution requires IEEE permission. See http://www.ieee.org/publications_standards/publications/rights/index.html for more information.
Authorized licensed use limited to: University Library Utrecht. Downloaded on October 21,2020 at 08:15:30 UTC from IEEE Xplore. Restrictions apply.

This article has been accepted for publication in a future issue of this journal, but has not been fully edited. Content may change prior to final publication. Citation information: DOI 10.1109/TTE.2020.3028784, IEEE Transactions on Transportation Electrification

[23] X. Tang, K. Liu, X. Wang, F. Gao, J. Macro, W. D. Widanage, "Model Migration Neural Network for Predicting Battery Aging Trajectories," *IEEE Transactions on Transportation Electrification*, vol. 6, no. 2, pp. 363-374, 2020.
[24] X. Li, L. Zhang, Z. Wang, P. Dong, "Remaining useful life prediction for lithium-ion batteries based on a hybrid model combining the long short-term memory and Elman neural networks," Journal of Energy Storage, vol. 21, pp. 510-518, 2019.
[25] B. Wu, V. Yufit, Y. Merla, R. F. Martinez-Botas, N. P. Brandon, G. J. Offer, "Differential thermal voltammetry for tracking of degradation in lithium-ion batteries," Journal of Power Sources, vol. 273, pp. 495-501, 2015.
[26] X. Li, C. Yuan, Z. Wang, "State of health estimation for Li-ion battery via partial incremental capacity analysis based on support vector regression," Energy, vol. 203, pp. 117852, 2020.
[27] X. Tang, C. Zou, K. Yao, J. Lu, Y. Xia, F. Gao, "Aging trajectory prediction for lithium-ion batteries via model migration and Bayesian Monte Carlo method," *Applied Energy*, vol. 254, pp. 113591, 2019.
[28] Y. Li, M. Abdel-Monem, R. Gopalakrishnan, M. Berecibar, E. Nanini-Maury, N. Omar, P. van den Bossche, J. Van Mierlo, "A quick on-line state of health estimation method for Li-ion battery with incremental capacity curves processed by Gaussian filter," Journal of Power Sources, vol. 373, pp. 40-53, 2018.
[29] L. Wang, D. Lu, Q. Liu, L. Liu, X. Zhao, "State of charge estimation for LiFePO4 battery via dual extended kalman filter and charging voltage curve," Electrochimica Acta, vol. 296, pp. 1009-1017, 2019.
[30] C. Weng, Y. Cui, J. Sun, H. Peng, "On-board state of health monitoring of lithium-ion batteries using incremental capacity analysis with support vector regression," Journal of Power Sources, vol. 235, pp. 36-44, 2013.
[31] Y. Li, C. Zou, M. Berecibar, E. Nanini-Maury, J. C. W. Chan, P. van den Bossche, J. Van Mierlo, N. Omar, "Random forest regression for online capacity estimation of lithium-ion batteries," Applied Energy, vol. 232, pp. 197-210, 2018.
[32] Y. Merla, B. Wu, V. Yufit, N. P. Brandon, R. F. Martinez-Botas, G. J. Offer, "Extending battery life: A low-cost practical diagnostic technique for lithium-ion batteries," Journal of Power Sources, vol. 331, pp. 224-231, 2016.
[33] Y. Merla, B. Wu, V. Yufit, N. P. Brandon, R. F. Martinez-Botas, G. J. Offer, "Novel application of differential thermal voltammetry as an in-depth state-of-health diagnosis method for lithium-ion batteries," Journal of Power Sources, vol. 307, pp. 308-319, 2016.
[34] K. Goebel, B. Saha, A. Saxena, J. R. Celaya, J. P. J. I. i. Christophersen, m. magazine, "Prognostics in battery health management," vol. 11, no. 4, 2008.
[35] A. Savitzky, M. J. E. Golay, "Smoothing and Differentiation of Data by Simplified Least Squares Procedures," Analytical Chemistry, vol. 36, no. 8, pp. 1627-1639, 1964.
[36] W. S. Cleveland, E. Grosse, W. M. Shyu, Local regression models, in: Statistical models in S, Routledge, 2017.
[37] C. E. Rasmussen, Gaussian processes in machine learning, in: Advanced lectures on machine learning, Springer, 2004.
[38] G. O. Sahinoglu, M. Pajovic, Z. Sahinoglu, Y. Wang, P. V. Orlik, T. Wada, "Battery State-of-Charge Estimation Based on Regular/Recurrent Gaussian Process Regression," IEEE Transactions on Industrial Electronics, vol. 65, no. 5, pp. 4311-4321, 2018.
[39] G. O. Sahinoglu, M. Pajovic, Z. Sahinoglu, Y. Wang, P. V. Orlik, T. Wada, "Battery State-of-Charge Estimation Based on Regular/Recurrent Gaussian Process Regression," IEEE Transactions on Industrial Electronics, vol. 65, no. 5, pp. 4311-4321, 2018.
[40] X. Tang, F. Gao, C. Zou, K. Yao, W. Hu, T. Wik, "Load-responsive model switching estimation for state of charge of lithium-ion batteries," *Applied Energy*, vol. 238, pp. 423-434, 2019..
[41] J. Yang, B. Xia, W. Huang, Y. Fu, C. Mi, "Online state-of-health estimation for lithium-ion batteries using constant-voltage charging current analysis," Applied Energy, vol. 212, pp. 1589-1600, 2018.

Zhenpo Wang (M'11) received the Ph.D. degree in automotive engineering from the Beijing Institute of Technology, Beijing, China, in 2005.
He is currently a Professor with the School of Mechanical Engineering, Beijing Institute of Technology, and the Director of National Engineering Laboratory for Electric Vehicles. He has authored or coauthored four monographs and translated books as well as more than 80 technical papers. He also holds more than 60 patents. His current research interests include pure electric vehicle integration, packaging and energy management of battery systems, and charging station design.
Prof. Wang is the recipient of numerous awards including the Second National Prize for Progress in Science and Technology and the First Prize for Progress in Science and Technology from the Ministry of Education, China, and the Second Prize for Progress in Science and Technology from Beijing Municipal, China.

Changgui Yuan received the B.E. degree in automotive engineering from Tsinghua University, Beijing, China, in 2018. He is currently working toward the Master's degree in the National Engineering Laboratory for Electric Vehicles, School of Mechanical Engineering, Beijing Institute of Technology, Beijing, China.
His research interests include state estimation and fault diagnosis of lithium-ion batteries.

Xiaoyu Li (S'19) is currently pursuing the Ph.D. degree in the National Engineering Laboratory for Electric Vehicles, School of Mechanical Engineering, Beijing Institute of Technology, Beijing, China. His research interests include modeling, simulation, and control with algorithm design for state estimation and fault diagnosis of lithium-ion batteries.
Mr. Li has been a recipient of the National scholarship in 2019, and Outstanding Doctoral Candidate Cultivating Foundation of Beijing Institute of Technology in 2019, 2020. He is also serving as the reviewer for many excellent journals in the research field including IEEE TRANSACTIONS ON TRANSPORTATION ELECTRIFICATION, IEEE TRANSACTIONS ON POWER ELECTRONICS, JOURNAL OF POWER SOURCES, and ENERGY.

2332-7782 (c) 2020 IEEE. Personal use is permitted, but republication/redistribution requires IEEE permission. See http://www.ieee.org/publications_standards/publications/rights/index.html for more information.
Authorized licensed use limited to: University Library Utrecht. Downloaded on October 21,2020 at 08:15:30 UTC from IEEE Xplore. Restrictions apply.